Journal of Contaminant Hydrology 221 (2019) 98–107

Contents lists available at ScienceDirect

Journal of Contaminant Hydrology

journal homepage: www.elsevier.com/locate/jconhyd

Investigation of transient freshwater storage in island aquifers

Vivek S. Bedekar[a,b], Sama S. Memari[c], T. Prabhakar Clement[c,*]

[a] Department of Civil Engineering, Auburn University, Auburn, AL, USA
[b] S.S. Papadopulos & Associates, Inc., Bethesda, MD, USA
[c] Department of Civil, Construction and Environmental Engineering, University of Alabama, Tuscaloosa, AL, USA

ARTICLE INFO

Keywords:
Saltwater intrusion
Strip islands
Transient freshwater lens
Transient saltwater wedge
Island aquifers
Recharge cycles

ABSTRACT

Fresh groundwater in an island aquifer is an extremely important resource that is highly vulnerable to variations in natural weather cycles and climate change effects. On small islands, precipitation creates subsurface freshwater lenses that float on top of coalesced saltwater that has intruded from the surrounding seawater. The volume and shape of these highly vulnerable freshwater lenses depend on the size and shape of the island, underlying geology, and the rate and duration of groundwater recharge. This study focuses on the transient changes in freshwater storage volume within these lenses. We completed a sand tank experiment to visualize an evolving freshwater lens that undergoes a dry- and -wet recharge cycle resulting in forming a shrinking and an expanding lens. The physical experiments provided a dataset to develop a robust numerical model that can rigorously simulate different types of evolving transient freshwater lenses. Our laboratory data along with past literature information have indicated that the shrinking of a freshwater lens occurred at a slower rate relative to an expanding freshwater lens. This aspect of a rather rapid freshwater volume recovery was investigated further using the numerical model by imposing cyclic recharge patterns to study the impacts of shortened recharge periods on freshwater storage in island aquifers. The results show that a sustainable dynamic equilibrium condition can be achieved within a few cycles of periodic recharge. Unsustainable conditions were only encountered at extremely short recharge periods. The model was then extended to simulate a freshwater lens in Dauphin Island, Alabama, to assess changes in freshwater storage under realistic wet and dry recharge cycles. The experimental data together with the modeling results presented in this study provide a better understanding of transient changes in freshwater storage patterns in small islands.

1. Introduction

According to estimates by the United Nations, the Small Island Developing States (SIDS) have a combined population of about 65 million (UN-OHRLLS, 2015). Most of these islands have a limited amount of surface storage potential to capture freshwater and therefore groundwater aquifers are critical water resources in these islands. On several of these islands, streams and lakes are simply non-existent, hence the local groundwater has to be optimally used to support the needs of local communities, agriculture, and also to support the local tourism industry that could be a major source of income for these tropical islands (Custodio and Bruggeman, 1987; Díaz Arenas and Huertas, 1986).

Freshwater recharge entering into a typical strip island aquifer will float over the intruded dense saltwater, forming a lens (see Fig. 1). The extent of this freshwater lens will depend on the geology, recharge, and the shape and size of the island. Changes in precipitation patterns due to climate change effects and sea level rise can adversely impact the size and shape of the freshwater lens which, in many cases, could be the only source of potable water in small islands (Falkland and Custodio, 1991). Therefore, understanding the transient behavior of these freshwater lenses is vital for optimally managing the limited amount of fresh groundwater available in these islands.

Since the mid-1960s, due to industrialization and rapid population growth, freshwater in small islands has been depleted and hence small island aquifers have become the focus of several theoretical and field investigations. Researchers have presented analytical and semi-analytical solutions for predicting the location of saltwater-freshwater interface in coastal aquifers including islands (Henry, 1960; Henry, 1964; Fetter, 1972; Ketabchi et al., 2014). Numerical models have also been used by researchers to study freshwater lens beneath oceanic strip islands; for example, Anderson (1976) used a predictor-corrector technique to develop a finite difference model for predicting unsteady flow in a freshwater lens beneath an oceanic strip island; Underwood et al.

* Corresponding author.
E-mail address: pclement@ua.edu (T.P. Clement).

https://doi.org/10.1016/j.jconhyd.2019.02.004
Received 21 November 2018; Received in revised form 30 January 2019; Accepted 4 February 2019
Available online 06 February 2019
0169-7722/ © 2019 Elsevier B.V. All rights reserved.

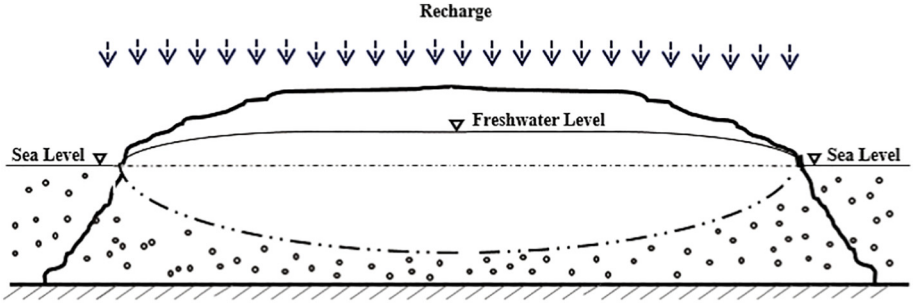

Fig. 1. Schematic of a freshwater lens in a strip island.

(1992) analyzed a two-layer atoll island and concluded that mixing of freshwater and saltwater occurs primarily as a result of oscillating vertical flow due to tidal fluctuations. Other studies have focused on field observations on islands. Wheatcraft and Buddemeier (1981) collected field data in Enjebi Island located within Enewark Atoll; Ayers and Vacher (1986) presented a detailed hydrogeological study of a small island called Deke on Pingelap Atoll located within the Eastern Caroline Islands; Presley (2005) studied the effects of the 1998 drought on Majuro Atoll, Marshall Islands; and Duncan (2011) provided a vulnerability assessment of fourteen developing Pacific Island Countries. UN-OHRLLS (2015) investigated the vulnerability of various freshwater resources in small islands, particularly to changes in precipitation patterns and prolonged drought conditions and pointed out the importance of rainwater harvesting in developing sustainable water resources in island aquifers.

Researchers have also developed several physical and mathematical models to study the freshwater flow processes near a saltwater wedge in coastal aquifers (e.g., Chang and Clement, 2013; Chang et al., 2011; Goswami and Clement, 2007; Gulley et al., 2016; Michael et al., 2005; Robinson et al., 2007). However, almost all of these efforts involve a uniform freshwater flow system with a single saltwater wedge intruding from the coastal boundary. In recent years, studies have investigated freshwater lenses bounded by double wedges in idealized sand-tank models (Stoeckl and Houben, 2012; Stoeckl et al., 2016). Stoeckl et al. (2016) provided a benchmark analysis employing the Simpson and Clement (2003) coupled-uncoupled approach to establish that double-wedge problems are highly worthy benchmark problems for testing density-coupled flow codes. Dose et al. (2014) investigated the steady-state interface geometry of freshwater lenses in layered aquifers. Stoeckl et al. (2015) investigated groundwater age stratification and travel times in a non-homogeneous island aquifer. Houben et al. (2018) demonstrated, using physical and numerical experiments, the influence of discrete and spatially distributed heterogeneity on forming unique distribution of saltwater interface.

Climate change effects can dramatically change the rainfall patterns worldwide, increasing the annual rainfall variability of many islands (Duncan, 2011; UN-OHRLLS, 2015). Furthermore, large-scale, ocean-atmospheric cyclical events such as El Niño and La Niña could force periodic dry and wet hydrological cycles. Extreme events, such as extended droughts, resulting from the coupling of these ocean-atmosphere cycles with climate change could potentially lead to extremely low recharge and even zero recharge during lengthy drought periods (Duncan, 2011; Falkland, 1992; UN-OHRLLS, 2015). For example, during the 1982–83 El Niño event rainfall in many parts of western Pacific was only 10–30% of the long-term average (Falkland, 1992). These extreme drought events could induce severe saltwater intrusion in island aquifers and this can adversely impact the highly vulnerable population living in these islands. The consequences of such extreme dry and wet cycles are difficult to predict. For example, it is currently unclear whether rainfall events resulting from wet cycles would be able to fully reverse the adverse impacts of dry cycles and reestablish a productive freshwater lens.

In published literature, there have been a few studies that examine the temporal changes in the saltwater interface after a dry and wet recharge cycle. Chang and Clement (2013) studied the movement of saltwater wedge and identified the asymmetry in intruding and receding saltwater wedges after a dry and wet cycle. Stoeckl and Houben (2012) and Stoeckl et al. (2016) examined the asymmetry between the time needed for the change in the height of saltwater interface during the development and depletion of the freshwater lens using both physical and numerical models. Lu and Werner (2013) used a numerical model to quantify the timescale associated with the saltwater wedge toe response in a confined aquifer system due to water level variations at the boundary and inland and developed empirical relations relating the changes in boundary head with toe locations. Abdoulhalik and Ahmed (2018) studied the transient motion of toe location of a single saltwater wedge using a physical tank model and simulated the data using a numerical model. The study examined the temporal response of saltwater interface using different hydraulic conductivity materials and also using different boundary conditions.

All aforementioned studies have investigated the temporal changes in saltwater wedge intrusion and retreating processes; however, none of these studies have quantified the changes in freshwater volume within islands or explored the temporal changes in freshwater storage patterns due to variations in recharge cycles. The objective of this study is to perform both qualitative and quantitative analyses of the temporal changes in the two-dimensional patterns of freshwater lens in strip islands, which are impacted by wet and dry recharge cycles. Both experimental and numerical modeling studies were completed to explore the temporal asymmetry between the freshwater lens depletion and lens formation under dry (no recharge) and wet (recharge) conditions. Additionally, in this study we investigated the impacts of cyclical weather patterns with extended drought periods on the freshwater availability in island aquifers. In order to extend the findings of the small scale tank studies to field scale, and to assess the timescale of transient processes under real-world precipitation and aquifer properties, a field-scale numerical model was developed. The model was used to conduct a numerical investigation for Dauphin Island, Alabama.

2. Methods

2.1. Laboratory methods

Fig. 2 shows the experimental sand tank model used in this study. The physical model was used to simulate the cross section of a strip island with ocean boundary at both sides. Freshwater input to the system was delivered through areal recharge, simulating the direct rainfall-induced recharge over the entire island aquifer. The dimension of the plexi-glass tank is: 50 cm × 28 cm × 2.5 cm. The overall thickness of the experimental aquifer is much smaller than its length and width, hence the tank can be conceptualized as a two-dimensional aquifer system.

As shown in the figure, the flow tank has three distinct sections: a right-hand seaside chamber, a central porous media chamber and a left-

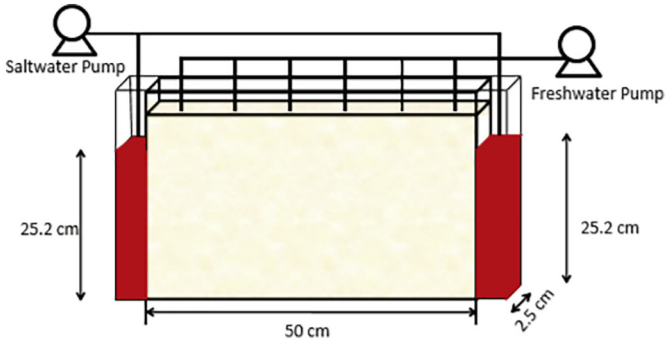

Fig. 2. Schematic of the laboratory setup.

hand seaside chamber. The central section was packed with uniform glass beads with average diameter of 1.1 mm. Hydraulic conductivity of the porous media was measured by creating a head gradient across the tank and measuring flow rate and head differences between the ends of the tank at various flow rates. The porous medium was packed under water by submerging the entire tank within a large water container. Glass beads were added layer by layer and each layer was compacted manually before adding the next layer. Packing the tank under submerged conditions helped prevent air bubbles getting trapped within the system. Constant head boundary conditions were maintained at both left and right seaside boundaries by continuously pumping dense water, simulating seawater, into the two chambers. The head in these chambers were maintained at a fixed level and the excess volume of seawater was allowed to overflow through multiple 1 mm diameter holes drilled in the side plates of the tank. The experimental method used was identical to the approach discussed in Goswami and Clement (2007). During our experiments, the measured values of constant head in the two chambers were 25.2 cm and 25.5 cm, for the dry (no recharge) and wet (recharge) cycles, respectively.

The denser water representing seawater was colored red using a food-grade dye; our previous investigations have shown that the dye used did not adsorb to the glass porous medium used in this study (Chang and Clement, 2013; Goswami and Clement, 2007). The saltwater was prepared using non-iodized salt, and the food dye was added at a ratio of about 50 mL per 20 L of saltwater. The density of the saltwater was measured using the ASTM 11H hydrometer, and the measured density of the colored saltwater was 1.016 ± 0.001 g/ml. The measured density of freshwater was 0.999 ± 0.001.

To simulate areal recharge, a multi-head peristaltic pump (Masterflex Tygon E-3603 pump) was used to deliver flow at 6 injection points. Before using the pump, the pumping rate of individual heads were measured and at different speeds to ensure uniform pumping. The total amount of recharge distributed from the six recharge points was 252 mL/min. The total area over which the recharge was applied was 50 cm × 2.5 cm, making the recharge rate equal to 2.016 cm/min. The recharge tubes were placed on the top of a porous media chamber at distances of 4.2 cm, 12.5 cm, 20.8 cm, 29.1 cm, 37.4 cm and 45.7 cm away from the left boundary. A porous cotton cloth was placed at the top of the porous media chamber to uniformly distribute the recharged water over the entire area of the aquifer. The experiments were recorded using a digital camera, and the pictures were later post-processed to map wedge locations and to calculate freshwater lens volumes.

The first set of experiments were conducted under uniform areal recharge conditions (2.016 cm/min) to simulate an initial steady-state wedge. Later, two different dry and wet stress periods were applied to the sand tank system to induce transient conditions. The dry stress period started at 0 min and lasted for 45 min; during this period, the areal recharge was turned off to allow the red-colored denser saltwater to intrude into the sand tank from both sides, allowing us to record the shrinking phase of the freshwater lens under dry conditions. After 45 min, the wet stress period was started by turning on the areal recharge (recharge flow was maintained at 2.016 cm/min) and system was allowed to evolve for another 45 min, allowing us to record the redevelopment phase of the freshwater lens under wet recharge conditions.

2.2. Modeling methods

SEAWAT (Langevin et al., 2008), a three-dimensional variable-density groundwater flow and transport simulation code, was used to develop a numerical model for this study. To simulate the two-dimensional flow tank experiment, the numerical model was discretized into 50 layers, 1 row, and 102 columns to represent the tank with dimensions 25 cm in height and 50 cm in width. The two model columns at both ends were used for specifying the lateral boundary conditions. Layers and columns were discretized with 0.5 cm grid spacing, with the exception of model layer 1, the top layer, that represents the water table layer. The top layer was assigned a thickness of 2.5 cm to accommodate the changes in phreatic surface levels and to simulate unconfined flow conditions.

An average uniform hydraulic conductivity value of 1050 m/day, which was measured in the laboratory, was assigned to the entire model domain. The confined storage coefficient was assumed to be negligible and was set to a very low value of 10^{-7}. Porosity value was set to be equal to 0.39, which was the average measured value-. The left and right boundaries of the model were imposed as prescribed head and prescribed concentration boundaries. A uniform recharge boundary was imposed at the top, and the bottom face of the model was simulated as a no flow boundary. The densities of freshwater and saltwater were set to 999 and 1016 kg/m^3, respectively. Assuming a concentration of 35 kg/m^3 for the red-colored denser seawater (which is close to the actual seawater concentration), the slope of the linear equation of state that relates of density and concentration ($\partial\rho/\partial C$) was estimated to be 0.4857. Note, in SEAWAT any arbitrary concentration value can be assumed provided an appropriate density slope value is calculated and used to simulate consistent scaled concentration results.

Temporal discretization included three stress periods: (1) the initial period to simulate the initial-steady-state conditions with constant recharge; (2) a transient forty-five minutes period without recharge (zero recharge to simulate dry conditions); and (3) a transient period with uniform recharge (to simulate wet conditions). For the three stress periods, prescribed head values at the lateral boundaries were set at 25.5 cm, 25.2 cm, and 25.5 cm, respectively; and recharge was set at 2.016 cm/min for the first and third stress period and zero for the second stress period. For numerical stability, flow and transport were tightly coupled with equal flow and transport time-step sizes, set at 0.54 s. SEAWAT uses a generalized conjugate gradient solver to solve the linear system of equations for dispersion, sources, and sinks. The total variation diminishing (TVD) scheme was used as the advection solution scheme, which calculates the time-step size honoring the Courant number (Cr) constraint of $Cr \leq 1$. The numerical model was later extended to simulate the impacts of cyclical wet-dry conditions on the experimental system. In addition, we also present a real-world modeling study that simulated a freshwater lens in Dauphin Island, Alabama to assess realistic timescales of freshwater volume change. The model parameters used in this study are discussed in detail in the case study section.

3. Results and discussion

3.1. Steady-state experimental conditions

Fig. 3a shows the symmetric salt wedges obtained under steady-state conditions. To obtain these steady-state profiles, the aquifer was originally filled with freshwater and then forced with saltwater boundary conditions; this was accomplished by replacing the

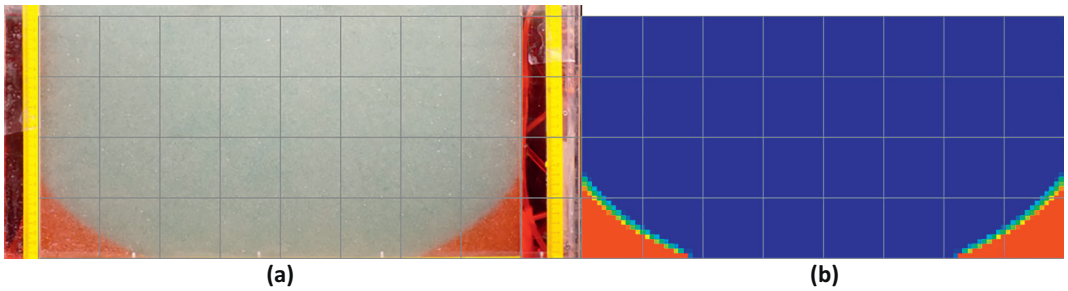

Fig. 3. Steady-state saltwater profile (*red represents saltwater*): (a) laboratory observation; and (b) simulated results. (For interpretation of the references to colour in this figure legend, the reader is referred to the web version of this article.)

freshwater in the left and right reservoirs with seawater by pumping excess amount of saltwater. The saltwater head at the two boundaries were maintained at a constant level and the recharge from the top remained zero. These conditions allowed red-colored saltwater to rapidly intrude from both sides into this recharge-free freshwater aquifer. After about 10 min of intrusion, the recharge pumps were turned on to maintain a constant flow rate of 2.016 cm/min, which was uniformly distributed over the top of the aquifer. The recharged system was allowed to evolve for about an hour to reach the steady state condition shown in Fig. 3a. These wedge profiles were set as the base case initial condition in this experimental study. At this steady state condition, the freshwater recharge supplied from the top fully balanced the saltwater forced from the boundaries forming two symmetric wedges.

Fig. 3b shows the steady-state conditions simulated using the SEAWAT model. The model was developed using the measured experimental parameters and it was run for a long time starting with a freshwater state as the initial condition. Fig. 3b shows the model simulated steady-state profile. In the model, the top layer was simulated as an unconfined layer and all other internal lower layers were assumed as confined layers. The model was run in a predictive mode using low longitudinal and transverse dispersivity values of 0.01 and 0.001 cm, respectively. These values are similar to the values used in other experimental studies to simulate similar type of sharp saltwater wedges (Abarca and Clement, 2009; Chang and Clement, 2012; Goswami and Clement, 2007). Preliminary sensitivity simulations completed using higher dispersivity values indicated that use of larger dispersivity values induced more dispersion than what was observed in the system. Larger dispersivitiy values in the simulations resulted in a more vertical saltwater wedge during saltwater intrusion. Comparison of Fig. 3a and Fig. 3b results indicate excellent agreement between the experimental data and numerical results.

3.2. Transient experimental conditions

The steady state system discussed above was used as the initial condition to simulate two distinct transient flow conditions involving dry and wet recharge cycles. In order to simulate transient conditions, we first instantaneously shut the recharge pump to simulate a dry cycle. The no-recharge condition was allowed to evolve for 45 mins to simulate a dry period. Transient salt wedge profiles observed after 5, 10, 15, 25, 35 and 45 min are shown in the left panel of Fig. 4. As shown in Fig. 4a, in the initial steady system the recharge flow minimizes saltwater intrusion effects and the wedges intruded only to about 10.4 cm from both saltwater boundaries. Fig. 4b shows that once the recharge was stopped, the wedges started to rapidly intrude into the system from both sides and the toe of the wedge reached about 18.75 cm from the lateral boundary after 5 min of transport. After about 11 to 12 min of transport the two wedges started to coalesce close to the center of the tank, and Fig. 4c shows the fully merged wedge observed after 15 min. It is interesting to note that after coalescing, the wedges formed a “V shaped” profile with the lowest point located at about 6.25 cm from the bottom of the tank. With time, the wedge developed a “U-shaped” profile and the low point started to lift and was located at about 14, 18.5, and 20.3 cm from the bottom of the tank at 25, 35 and 45 min, respectively (see Fig. 4d, e and f). Note the true steady-state pattern for this no recharge condition will be a flat profile, and our preliminary experiments showed that it will take about 2 h to approach this flat steady state condition where the saltwater will fully intrude and replace the entire freshwater. However, in this experiment, we only maintained the zero-recharge condition for 45 mins.

To simulate the wet cycle, we turned on the recharge pump and supplied a uniform recharge at a rate of 2.016 cm/min, which was identical to the recharge used to simulate the base-case, steady-state wedge. The recharged water infiltrated into the aquifer and reestablished the freshwater lens by forcing the saltwater wedge to recede back toward the left and right seaside boundaries. The figures presented in the right panel of Fig. 4 show the transient movement of the receding wedge. Interestingly, the intruding and receding wedges have very different patterns. One of the major differences was that the intruding wedge initially formed a V-shaped profile that later evolved into a U-shaped profile; whereas, the receding wedge always had an elongated U-shaped profile. In the past, research studies have primarily focused on the toe location of the saltwater wedge. However, in our dry and wet cycle comparison analysis we integrated the area above the wedge to quantify the total amount of freshwater storage in the system to define the state of the system. The volume of water stored at any given time was then used to compare the differences in the overall shapes of intruding and receding saltwater wedges.

Fig. 4h shows the location of the receding wedge after receiving 5 min of recharge. The experimental data show that the system formed an elongated U-shaped wedge and the lower-most point of this wedge was located at about 12.3 cm from the bottom of the aquifer. Fig. 4i, j, and k show the wedge profiles observed after 15, 25, and 35 min of recharge (or 60, 70, and 80 total minutes), and the low points of the wedges were located about 4.2, 1.8 and 0.7 cm from the bottom of the tank for the three times, respectively. Fig. 4l shows that after 45 mins of recharge (or total experimental time of 90 min) the wedges were totally disconnected and the toes of the two disconnected wedges were located approximately 13.5 cm from the boundary (note the true steady-state location is about 10.4 cm).

The SEAWAT code was used to simulate this dataset and the model simulated profiles of the intruding and receding wedges are also shown in Fig. 4. These figures show that the model was able to closely reproduce the experimental observations. These results indicate that this stable-wedge problem has three states involving distinctly different types of salt wedge patterns including the traditional exponentially-decaying wedge, a V-shaped intruding wedge, and a U-shaped receding wedge. These data provide a unique set of transient wedge profiles which can be useful for benchmarking density-coupled flow models that involve stable interfaces (i.e., dense water present at the bottom).

To quantify the changes in freshwater storage patterns, the amount of freshwater in the tank experiments was computed by post processing

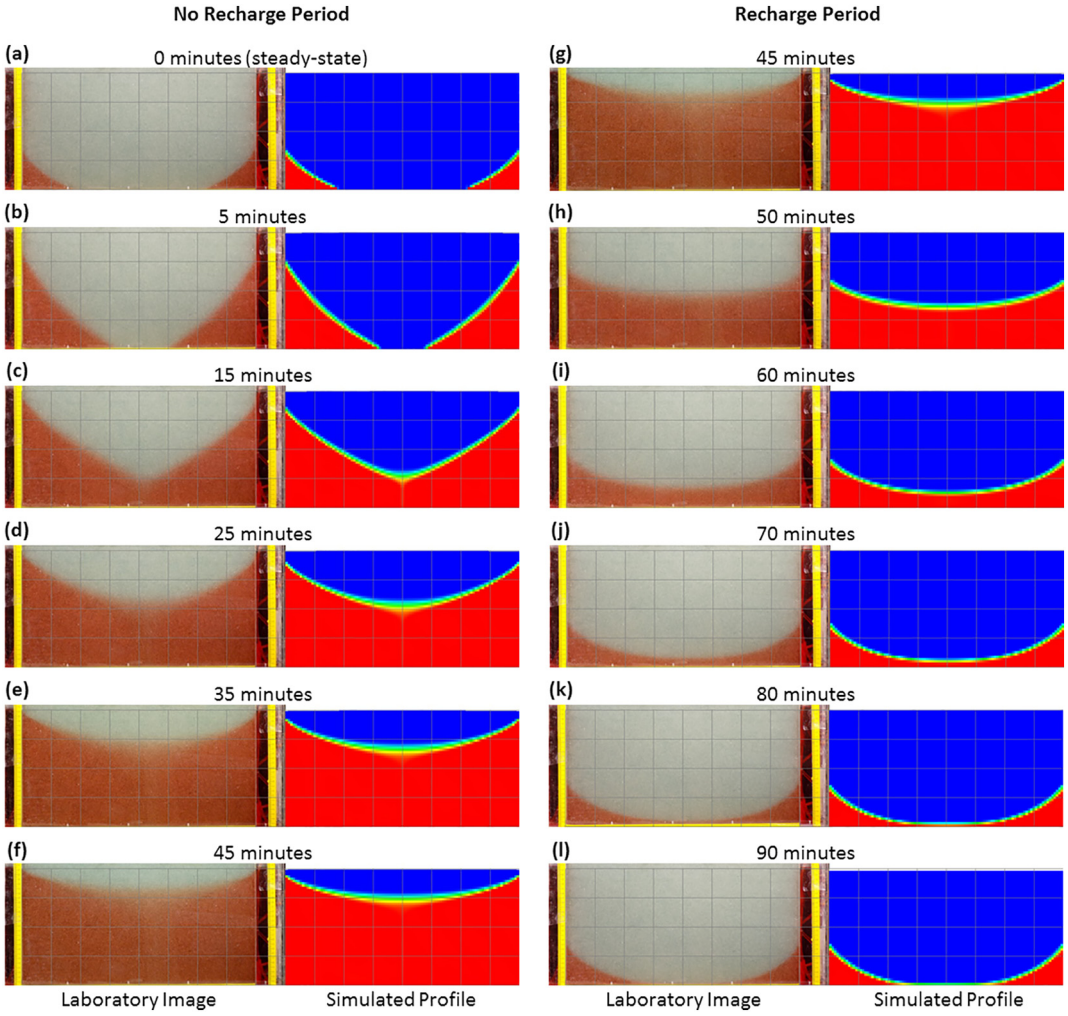

Fig. 4. Comparison of saltwater profiles observed in the experimental tank with model simulated results. The left side panels show data for 5 min to 45 min that represent transport under no recharge (dry) conditions during which the denser saltwater intruded into the system. The right side panels show data from 45 min to 90 min that represent transport under recharge (wet) conditions during which the recharged freshwater displaced the saltwater out of the system.

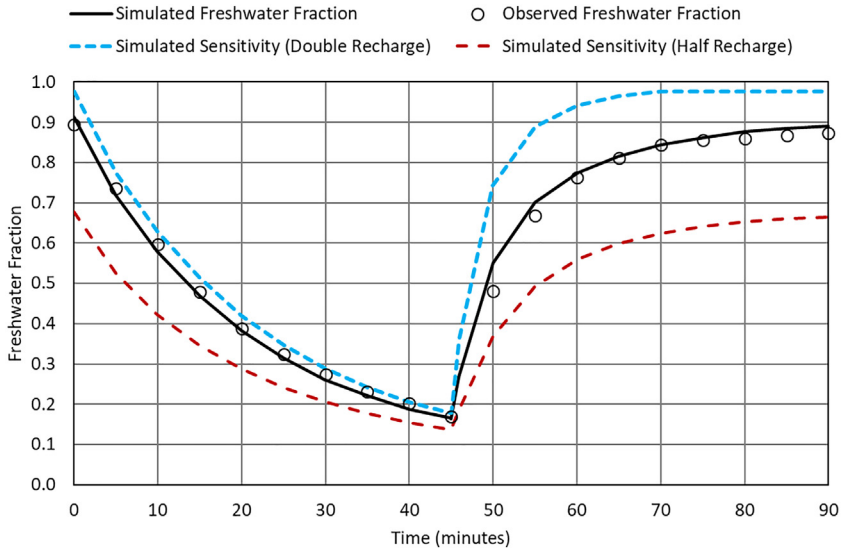

Fig. 5. Time series plot showing changes in freshwater storage. Note the storage volume is reported as a fraction of the total tank volume.

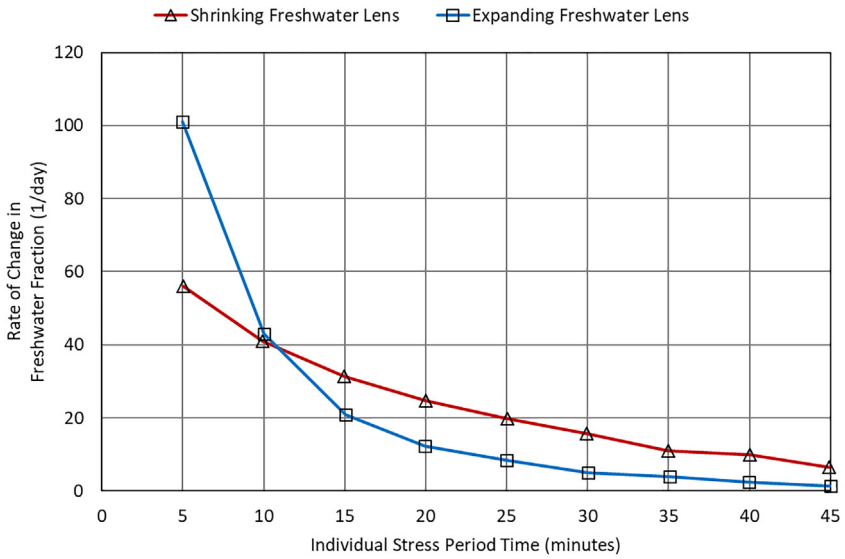

Fig. 6. Rate of change of freshwater fraction within the shrinking and expanding freshwater lenses. Note the x-axis represents individual stress period (dry or wet cycle) time.

the digital images to estimate the area above the wedge. The simulated freshwater fractions were delineated using a threshold of a normalized concentration of 0.25. The changes in the amount of freshwater stored within the system estimated for different times are summarized in Fig. 5. A good agreement is seen in simulated and observed changes in freshwater fractions. Fig. 5 also shows the sensitivity of freshwater fraction changes to recharge rate. The freshwater recovery is most sensitive to the recharge rate, and it is seen that the rate of recovery increases with the increase in the recharge intensity. The asymmetry observed between depletion and recovery cycles is enhanced with a higher recharge rate. For the base simulation the figure shows that during both dry and wet cycles the greatest change in the freshwater volume occurred during the inception of the transient period (this can also be seen in Fig. 4). As time progressed, the rate of change of net freshwater storage decreased considerably. Fig. 6 shows the absolute rate of change of freshwater storage observed during the dry and wet stress periods. For visual comparison, both the rate of decrease and increase in freshwater volume is plotted as the absolute value on the positive y-axis. These rates were calculated as the change in the freshwater fraction over time interval divided by the length of time interval over which the change occurred. When we compared these rates of storage change data for both dry and wet cycles during the first 10 min, the rate of change is high for the expanding freshwater lens which was accumulating water under receding saltwater wedge conditions during the wet period. Our estimations show that during the dry period, the freshwater fraction decreased by 33% (of the total storage) within 10 min; on the other hand, during the wet period, the storage increased to about 53% within 10 min. At the beginning of the wet period the recovery rate was almost double as compared to the depletion rate at the onset of the dry period. However, after the initial surge in freshwater storage, the rate of change slowed down as the freshwater forced the intruded saltwater to split into two separate wedges.

Chang and Clement (2012) discuss potential reasons for the observed asymmetry between intruding and receding wedges. Based on their findings one can postulate that the asymmetry observed in the time scales of shrinking and expanding freshwater lens can be attributed to the velocity variations occurring within the saltwater wedge during intruding and receding conditions. During intrusion (or shrinking freshwater lens conditions), saltwater flow from the lateral boundary is moving inward within the saltwater wedge, which will be opposite to the outward freshwater flow occurring within the lens. The freshwater flow will eventually exit through the lateral boundary within a narrow area close to the top of the tank. On the contrary, during recession (or expanding freshwater lens conditions), both freshwater and saltwater flows will align to move toward the lateral boundary and the entire lateral boundary area will be available for outflow; these well aligned processes facilitate the saltwater recession to occur at a much higher rate as compared to intrusion.

These results imply that the freshwater volume stored within a strip island will recover and accumulate water rather rapidly during the initial phase of a rainfall event, when compared to the freshwater volume lost during the initial phase of a drought event. Overall, these results show a unique emerging pattern where natural systems can potentially manage water storage rather efficiently. The findings observed in the laboratory-scale experiments were extended to a field-scale investigation using a numerical model representing a realistic system in Dauphin Island, Alabama. The field-scale investigation uses real-world spatial domain, precipitation data and aquifer parameters, and the model was used to observe expected time scale differences in asymmetric transient processes and these results are discussed in Section 3.4.

3.3. Understanding freshwater sustainability under variable recharge conditions

The observations made in the experimental study where the freshwater lens recovery process was found to be relatively faster than depletion led us to conduct further numerical simulations for the experimental system for cyclic wet-dry conditions. Cyclic wet-dry conditions were simulated using multiple stress periods. Steady-state conditions were simulated under constant recharge conditions as the first stress period. Dry conditions were invoked by implementing zero-recharge during even numbered stress periods, and recharge was implemented in subsequent odd numbered stress periods to represent wet conditions. One cycle of wet-dry conditions, therefore, comprised of two consecutive stress periods, one without recharge followed by one with recharge. Six such wet-dry cycles were simulated. The dimensions of the numerical model used for these simulations were the same as the sand tank model. The duration representing dry conditions in all simulations was set to a constant time of 25 min. However, the duration of wet periods was allowed to vary in different simulations. Note that the recharge rate was the same in all simulations and only the duration was varied.

For the first simulation, the recharge period was set to ten minutes,

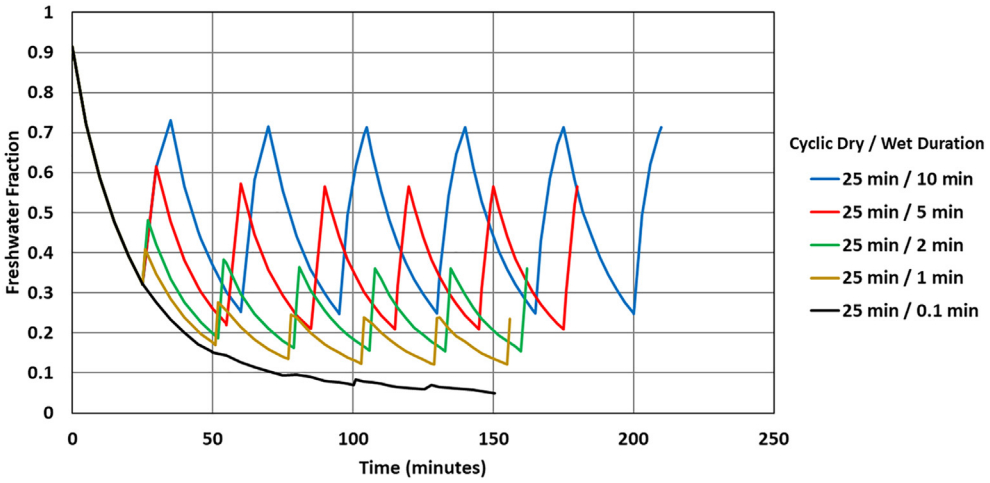

Fig. 7. Time series plot showing changes in freshwater storage for cyclic wet-dry simulations. Each simulation considers six cycles of wet and dry periods. A cycle comprises of a 25-min dry period and varying duration of wet periods from one simulation to the other. The total time of each simulation varies depending on the duration of its wet period.

which resulted in a wet-dry cycle which was 35 min long comprising of a 25-min dry period followed by 10 min of wet recharge period. Six such cycles were employed in all these simulation experiments. For the second simulation, the duration of wet period was reduced to 5 min and a dry period was set to 25 min; therefore, the duration of each cycle in the second simulation was 30 min. In subsequent simulations the recharge period was reduced to 2 min, 1 min, and 0.1 min. The last simulation with a wet period duration of 0.1 min was considered as an extreme case of recharge period.

Fig. 7 shows the time-series plots for all five cyclical wet-dry scenarios. The results show that the freshwater volumes decrease from one simulation to the other as the duration of wet period was decreased. Within every simulation experiment (which consisted for six cycles), a dynamic equilibrium was achieved after about three wet-dry cycles; i.e., the freshwater volume roughly changed by the same amount after three cycles. The only exception to that is the extreme case of a recharge duration of one-tenth of a minute; in this case, the freshwater volume continued to decrease after every cycle.

Fig. 8 shows the cyclic change in the maximum freshwater achieved at the end of each wet-dry cycle. The shape of the curve for each simulation stabilizes within a few wet-dry cycles indicating that a dynamic equilibrium is achieved, but with different freshwater volumes. The higher the duration of recharge, the higher is the freshwater volume achieved at the dynamic equilibrium condition. For example, with a 25-min dry and a 10-min wet cycle, the maximum freshwater volume fraction under a dynamic equilibrium condition is found to be 0.71. Note the freshwater volume fraction indicates the fraction of system that is occupied by freshwater. For a simulation with recharge period as low as 1-min and with a dry period of 25 min, the maximum freshwater fraction is 0.24 at the dynamic equilibrium condition. As seen in Figs. 7 and 8, a sustained freshwater volume level was attained for simulations in which recharge occurred as briefly as for 1-min after a 25-min dry period. Only when the recharge duration was shortened to a tenth of a minute (with a 25-min dry period) the freshwater lens became unsustainable. These results show that the freshwater recharge accumulated even during short recharge cycles can help sustain freshwater storage during extended dry periods.

3.4. Case study for Dauphin Island, Alabama

A field-scale study was completed to assess the real-world implication of the observations made in this experimental study. Dauphin Island is located at the southwest end of Alabama in the US was selected for this example. The western end of the island, which has an elongated strip of land of approximately 20 km long with an average width of approximately 400 m, was used as the model domain. This island region is ideally suited for simulating conditions on an infinite strip island. A cross-sectional model of the strip of land was created to assess changes in freshwater lens volumes. Parameterization of the field model was based on a modeling study of Dauphin Island presented by Chang et al. (2016). The 400 m width of the strip was discretized into 160 model cells using a 2.5 m horizontal discretization. The depth of the model

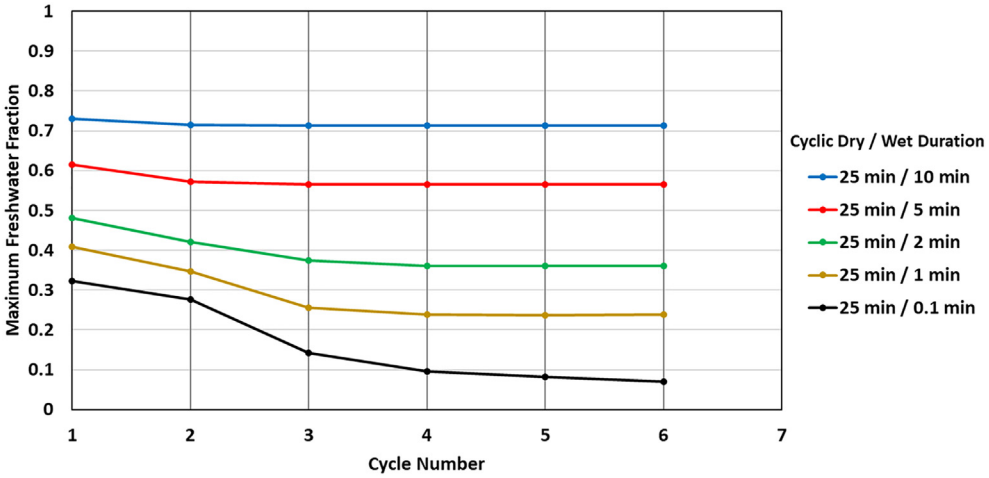
Maximum Freshwater Fraction
Cycle Number
Cyclic Dry / Wet Duration
25 min / 10 min
25 min / 5 min
25 min / 2 min
25 min / 1 min
25 min / 0.1 min

Fig. 8. Time series plot showing maximum freshwater storage within each wet-dry cycle. Six cycles were simulated for each simulation. The total duration of each simulation is different and is based on the duration of the wet period for that simulation.

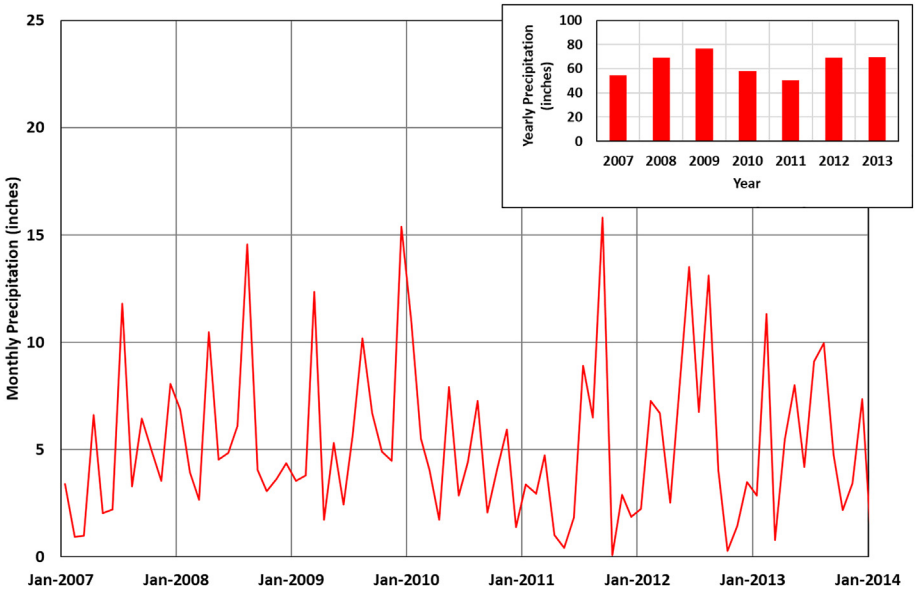

Fig. 9. Precipitation data from Mobile Regional Airport, Alabama, used for Dauphin Island model. Monthly precipitation is shown as a time-series plot and the inset shows yearly precipitation.

Table 1
Model parameters used for Dauphin Island simulation (reproduced from Chang et al., 2016).

Parameter	Sandy upper unit	Clay lower unit
Horizontal hydraulic conductivity	13.7 m/day	2.6×10^{-7} m/day
Vertical hydraulic conductivity	0.45 m/day	2.6×10^{-7} m/day
Specific storage	3.3×10^{-4} m^{-1}	3.3×10^{-3} m^{-1}
Longitudinal dispersivity	0.0001 m	
Transverse dispersivity	0.00001 m	
Saltwater concentration	35 kg/m^3	
Saltwater density	1025 kg/m^3	
Freshwater density	1000 kg/m^3	
Density slope	0.714	
Porosity	0.3	

was selected as 21 m, the top hydrogeologic unit being 13 m thick representing Holocene Sand underlain by a 7 m thick clay unit (Chang et al., 2016). The model grid was discretized vertically into 42 layers with a uniform vertical spacing of 0.5 m.

Real-world field conditions and rainfall data were used to simulate the freshwater lens in Dauphin Island, Alabama, to illustrate the differences in the rate of decrease and the rate of increase in freshwater volumes. Precipitation data was obtained for Mobile Regional Airport, Alabama, available from NOAA's National Climatic Data Center (NCDC). Monthly calculated precipitation rates used for generating transient groundwater recharge for the model is shown in Fig. 9. Net groundwater recharge was set at 5% of the precipitation amount. The figure shows a large monthly variation in precipitation values. On a larger timescale, there was an extended drought period between 2010 and the first half of 2011, which occurred in between two relatively wet years of 2009 and 2012 (see inset plot in Fig. 9). Other site parameters were taken from the calibrated model parameters presented in a previously published study (Chang et al., 2016) and the data are summarized in Table 1. The objective of this field scale simulation was to test whether the laboratory-scale observations made were applicable for field-scale conditions. Specifically, to test whether the freshwater recharge rapidly accumulated during the short recharge cycles will be able to sustain freshwater storage during extended dry periods. A transient model was simulated for the period of 2007–2013. To isolate the impacts of recharge on the freshwater volumes, only recharge was varied on a monthly basis during the transient period. All other boundary conditions were held constant. Initial conditions were set as steady-state conditions with average 2007–2013 recharge.

Fig. 10 shows the monthly variation in freshwater volume fraction predicted by the model. The relative changes in freshwater volume largely follow the variation in recharge applied to the model. Freshwater volume increases with increased recharge and vice versa. The results show that increase in recharge causes the freshwater to increase within the same month. Decrease in recharge however, shows a delayed response in freshwater lens depletion; the recession limb of the freshwater lens took several months to manifest on the decrease in freshwater volumes during dry cycles. This pattern can be observed in almost all the events in which recharge drops but it is most prominent during the extended dry cycle beginning in 2010 and lasting through the middle of 2011. During this period, the decrease in freshwater volume is not as drastic as the decrease in recharge conditions. Intermittent increase in recharge even by a small amount of rain in 2010 helped slow down the decrease in freshwater lens volume through the entire year. On the other hand, a large increase in recharge during 2009, 2011, and 2012 is reflected by an almost instantaneous increase in freshwater volume. While the absolute change in freshwater volume may not be significant, it is interesting to note that, like the laboratory-scale results, these field-scale simulations also show a delayed pattern of freshwater lens depletion relative to the freshwater lens formation.

The real-world example simulated here qualitatively demonstrates the delayed response of freshwater volume depletion over several months due to the decrease in recharge, and an almost instantaneous recovery of freshwater volume resulting from increased recharge. These observations highlight the importance of managing groundwater replenishment from even short rainfall events after or during an extended dry period. Efforts to capture recharge from these short rainfall events are consequential to better manage freshwater resources in island aquifers.

4. Conclusions

A laboratory experiment was conducted to study the patterns of a shrinking and expanding freshwater lens in an infinite strip island. The laboratory data were simulated using a numerical model developed using SEAWAT. The modeled results closely matched the experimental data. The data show asymmetry in the time scales of the shrinking and expanding freshwater lens. It was also observed that the initial period of

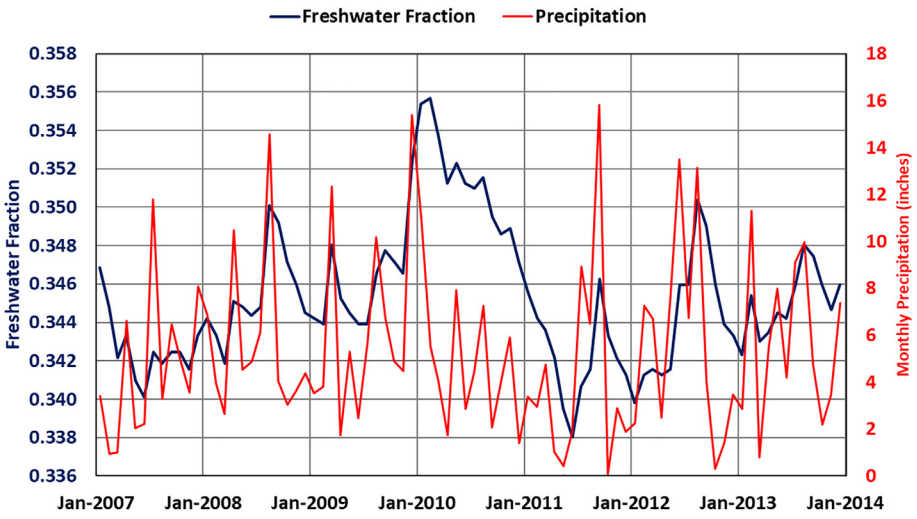

Fig. 10. Change in freshwater fraction for Dauphin Island model. Freshwater fraction is the volume of freshwater divided by the total volume of cross-section model. Precipitation is also plotted for comparison between change in precipitation and the induced change in freshwater volume fraction in the model.

stress causes the highest change in freshwater volume storage (both loss and gain) and the rate of change of freshwater storage rapidly decreases with the passage of time. Interestingly, the freshwater lens expansion (or accumulation of freshwater) during the early period of the wet cycle occurred at a greater rate when compared to the freshwater lens shrinkage (or loss of freshwater) rate during the dry cycle. These results show that natural systems could support an efficient non-linear feedback mechanism that has an emerging property where the groundwater system loses water slowly during a dry cycle but it can recover fast by gaining water rather rapidly during a wet cycle. This non-linear feedback mechanism and its implication on faster freshwater recovery greatly emphasizes the importance of implementing careful recharge management strategies to maximize freshwater storage in small island aquifers. Our experimental data as well as model simulation results show that even short duration rainfall events can greatly enhance the freshwater availability in small islands.

5. Acknowledgements

This work was, in part, supported by USGS Alabama Water Resources Competitive Grants Program. We are thankful to three anonymous reviewers for their valuable feedback in improving this paper. TPC developed the initial ideas and designed the experiments, developed funding and supervised the work. SSM designed and conducted the final set of experiments, VB developed the SEAWAT models, and both VB and TPC jointly analyzed the dataset. VB and TPC developed the initial draft of the manuscript and all three authors actively participated in finalizing the manuscript. Overall, all three authors have contributed to this effort and their relative responsibilities, computed using the Clement (2014) approach, are: VB (50%), SSM (20%) and TPC (30%).

References

Abarca, E., Clement, T.P., 2009. A novel approach for characterizing the mixing zone of a saltwater wedge. Geophys. Res. Lett. 36 (6).
Abdoulhalik, A., Ahmed, A.A., 2018. Transience of seawater intrusion and retreat in response to incremental water level variations. Hydrol. Process. 32 (17), 2721–2733.
Anderson, M., 1976. Unsteady groundwater flow beneath strip oceanic islands. Water Resour. Res. 12 (4), 640–644.
Ayers, J.F., Vacher, H., 1986. Hydrogeology of an atoll island: a conceptual model from detailed study of a micronesian example. Groundwater 24 (2), 185–198.
Chang, S.W., Clement, T.P., 2012. Experimental and numerical investigation of saltwater intrusion dynamics in flux controlled groundwater systems. Water Resour. Res. 48, W09527. https://doi.org/10.1029/2012WR012134.
Chang, S.W., Clement, T.P., 2013. Laboratory and numerical investigation of transport processes occurring above and within a saltwater wedge. J. Contam. Hydrol. 147, 14–24.
Chang, S.W., Clement, T.P., Simpson, M.J., Lee, K.K., 2011. Does sea-level rise have an impact on saltwater intrusion? Adv. Water Resour. 34 (10), 1283–1291.
Chang, S.W., Nemec, K., Kalin, L., Clement, T.P., 2016. Impacts of climate change and urbanization on groundwater resources in a barrier island. J. Environ. Eng. 142 (12).
Clement, T.P., 2014. Authorship matrix: a rational approach to quantify individual contributions and responsibilities in multi-author scientific articles. Sci. Eng. Ethics 20 (2), 345–361.
Custodio, E., Bruggeman, G.A., 1987. Groundwater problems in coastal areas. Stud. Rep. hydrol. 45.
Díaz Arenas, A., Huertas, J. Febrillet, 1986. Hydrology and water balance of small islands: a review of existing knowledge. In: Technical Documents in Hydrology. UNESCO.
Dose, E.J., Stoeckl, L., Houben, G.J., Vacher, H., Vassolo, S., Dietrich, J., Himmelsbach, T., 2014. Experiments and modeling of freshwater lenses in layered aquifers: steady state interface geometry. J. Hydrol. 509, 621–630.
Duncan, D., 2011. Freshwater Under Threat/Pacific Islands. *United Nations Environment Programme, Bankok*.
Falkland, A.C., 1992. Small Tropical islands: water resources of paradise last. In: *IHP Humid Tropics Programme series*: Unesco.
Falkland, A.C., Custodio, E., 1991. *Hydrology and Water Resources of Small Islands: a Practical Guide*: Unesco.
Fetter, C.W., 1972. Position of the saline water interface beneath oceanic islands. Water Resour. Res. 8 (5), 1307–1315.
Goswami, R.R., Clement, T.P., 2007. Laboratory-scale investigation of saltwater intrusion dynamics. Water Resour. Res. 43, W04418. https://doi.org/10.1029/2006WR005151.
Gulley, J., Mayer, A., Martin, J., Bedekar, V., 2016. Sea level rise and inundation of island interiors: assessing impacts of lake formation and evaporation on water resources in arid climates. Geophys. Res. Lett. 43 (18), 9712–9719.
Henry, H.R., 1960. Salt Intrusion into Coastal Aquifers. Columbia University, New York.
Henry, H.R., 1964. Effects of Dispersion on Salt Encroachment in Coastal Aquifers. U.S. Geological Survey Water-Supply Paper. pp. 1613–C.
Houben, G.J., Stoeckl, L., Mariner, K.E., Choudhury, A.S., 2018. The influence of heterogeneity on coastal groundwater flow-physical and numerical modeling of fringing reefs, dykes and structured conductivity fields. Adv. Water Resour. 113, 155–166.
Ketabchi, H., Mahmoodzadeh, D., Ataie-Ashtiani, B., Werner, A.D., Simmons, C.T., 2014. Sea-level rise impact on fresh groundwater lenses in two-layer small islands. Hydrol. Process. 28 (24), 5938–5953.
Langevin, C.D., Thorne, T.D., Dausman, A.M., Sukop, M.C., Guo, W., 2008. SEAWAT Version 4: a Computer Program for Simulation of Multi-Species Solute and Heat Transport.
Lu, C., Werner, A.D., 2013. Timescales of seawater intrusion and retreat. Adv. Water Resour. 59, 39–51.
Michael, H.A., Mulligan, A.E., Harvey, C.F., 2005. Seasonal oscillations in water exchange between aquifers and the coastal ocean. Nature 436 (7054), 1145–1148.
Presley, T.K., 2005. Effects of the 1998 Drought on the Freshwater Lens in the Laura Area. Republic of the Marshall Islands, Majuro Atoll.
Robinson, C., Li, L., Prommer, H., 2007. Tide-induced recirculation across the aquifer-ocean interface. Water Resour. Res. 43 (7).
Simpson, M.J., Clement, T.P., 2003. Theoretical analysis of the worthiness of Henry and Elder problems as benchmarks of density-dependent groundwater flow models. Adv. Water Resour. 26 (1), 17–31.
Stoeckl, L., Houben, G., 2012. Flow dynamics and age stratification of freshwater lenses: experiments and modeling. J. Hydrol. 458, 9–15.
Stoeckl, L., Houben, G.J., Dose, E.J., 2015. Experiments and modeling of flow processes in freshwater lenses in layered island aquifers: analysis of age stratification, travel times and interface propagation. J. Hydrol. 529, 159–168.

Stoeckl, L., Walther, M., Graf, T., 2016. A new numerical benchmark of a freshwater lens. Water Resour. Res. 52 (4), 2474–2489.
Underwood, M.R., Peterson, F.L., Voss, C.I., 1992. Groundwater lens dynamics of atoll islands. Water Resour. Res. 28 (11).
UN-OHRLLS, 2015. Small Island Developing States in Numbers: climate Change, 2015 ed. .
Wheatcraft, S.W., Buddemeier, R.W., 1981. Atoll Island Hydrology. Ground Water 19, 311–320.